



Published in final edited form as:

Clin Biomech (Bristol, Avon). 2016 January ; 31: 20–28. doi:10.1016/j.clinbiomech.2015.10.006.

USE OF SHEAR WAVE ULTRASOUND ELASTOGRAPHY TO QUANTIFY MUSCLE PROPERTIES IN CEREBRAL PALSY

Sabrina S.M. Lee^{1,2}, Deborah Gaebler-Spira^{1,2}, Li-Qun Zhang^{1,2}, William Z. Rymer^{1,2}, and Katherine M. Steele³

¹ Rehabilitation Institute of Chicago, Chicago, IL, USA

² Northwestern University, Chicago, IL, USA

³University of Washington, Seattle, WA, USA

Abstract

Background—Individuals with cerebral palsy tend to have altered muscle architecture and composition, but little is known about the muscle material properties, specifically stiffness. Shear wave ultrasound elastography allows shear wave speed, which is related to stiffness, to be measured *in vivo* in individual muscles. Our aim was to evaluate the material properties, specifically stiffness, as measured by shear wave speed of the medial gastrocnemius and tibialis anterior muscles in children with hemiplegic cerebral palsy across a range of ankle torques and positions, and fascicle strains.

Method—Shear wave speed was measured bilaterally in the medial gastrocnemius and tibialis anterior over a range of ankle positions and torques using shear wave ultrasound elastography in eight individuals with hemiplegic cerebral palsy. B-mode ultrasound was used to measure muscle thickness and fascicle strain.

Results—Shear waves traveled faster in the medial gastrocnemius and tibialis anterior of the more-affected limb by 14% ($p=0.024$) and 20% ($p=0.03$), respectively, when the ankle was at 90°. Shear wave speed in the medial gastrocnemius increased as the ankle moved from plantarflexion to dorsiflexion (less affected: $r^2=0.82, p<0.001$; more-affected: $r^2=0.69, p<0.001$) and as ankle torque increased (less affected: $r^2=0.56, p<0.001$; more-affected: $r^2=0.45, p<0.001$). In addition, shear wave speed was strongly correlated with fascicle strain (less affected: $r^2=0.63, p<0.001$; more-affected: $r^2=0.53, p<0.001$).

Interpretation—The higher shear wave speed in the more-affected limb of individuals with cerebral palsy indicates greater muscle stiffness, and demonstrates the clinical potential of shear

Corresponding author: Sabrina S.M. Lee, Department of Physical Therapy and Human Movement Sciences, Northwestern University, 645 N Michigan Avenue, Suite 1100, Chicago, IL, 60611, United States, s-lee@northwestern.edu, 312-503-4564.

Publisher's Disclaimer: This is a PDF file of an unedited manuscript that has been accepted for publication. As a service to our customers we are providing this early version of the manuscript. The manuscript will undergo copyediting, typesetting, and review of the resulting proof before it is published in its final citable form. Please note that during the production process errors may be discovered which could affect the content, and all legal disclaimers that apply to the journal pertain.

Conflict of interest statement

Dr. Li-Qun Zhang, the PI of the AACPDM research grant, holds an equity position in Rehabtek, which received NIH and NSF grants in developing the IntelliStretch rehabilitation robot used in this study.

wave elastography as a non-invasive tool for investigating mechanisms of altered muscle properties and informing diagnosis and treatment.

Keywords

cerebral palsy; muscle; ultrasound; shear wave elastography

1. Introduction

Cerebral palsy (CP) is the most common pediatric neuromuscular disorder, impacting roughly 3 out of every 1000 individuals (Yeargin-Allsopp et al., 2008). Movement and coordination are impaired among individuals with CP due to both altered neural control and secondary changes in muscle properties (Gage, 2009). These secondary changes in muscle are a primary target for treatment and commonly require expensive, invasive procedures for correction, such as multi-level orthopaedic surgery. Quantifying the magnitude and functional impact of changes in muscle properties for individual patients with CP remains challenging, and hinders treatment planning.

Changes in muscle properties have been documented at nearly every level of the hierarchical structure of muscle in individuals with CP. From the sub-microscopic level, where changes occur in myosin heavy chain isoforms (Ponten and Stal, 2007), sarcomere lengths (Smith et al., 2011), and fiber types (Ito et al., 1996), to the whole muscle level where volume, cross-sectional area, and thickness are reduced (Barber et al., 2011). Such changes in muscle properties are significant and may negatively impact movement. For example, the muscles' passive resistance to stretch is commonly increased in CP, contributing to perceived muscle contracture and limiting joint range of motion. Increases in muscles' passive resistance to stretch can be attributed to increased collagen of the extracellular matrix (ECM) (Booth et al., 2001; Friden and Lieber, 2003; Smith et al., 2011), and changes in structural (Magid and Law, 1985) and intracellular (Friden and Lieber, 2003; Lieber et al., 2003) proteins.

There is widespread acceptance that muscles' passive properties are altered in individuals with CP (Barber et al., 2011; Friden and Lieber, 2003; Smith et al., 2011); however, obtaining quantitative *in vivo* measurements to support this assertion remains a challenge. Prior non-invasive methods to evaluate muscle or joint stiffness, such as torque-angle measurements (Barber et al., 2011; Sinkjær and Magnussen, 1994), compression elastography (Park and Kwon, 2012), and tendon indentation (Chardon et al., 2010) have provided important measures in healthy individuals and those with impaired movements. By measuring the change in torque, as an estimate of change in force, and angle displacement, as an estimate of change in muscle length, during an external perturbation, estimates of muscle or joint stiffness can be obtained. Sinkjaer et al. (1988) developed a method where this stiffness could be distinguished as passive, intrinsic, and reflex-mediated stiffness (Sinkjær et al., 1988) and applied this method to the ankle extensors of hemiparetic patients (Sinkjær and Magnussen, 1994) and individuals with multiple sclerosis (Sinkjær et al., 1993). However, these prior methods have multiple limitations including limited quantitative accuracy, muscle specificity, repeatability, ease of use in the clinic, and/or cost-effectiveness. Invasive methods have also been used such as biopsy or intraoperative

measurements (Friden and Lieber, 2003; Smith et al., 2011); these provide invaluable information on stiffness mechanisms at the cellular and fiber level, but not at the whole muscle level where we are limited to measurements of passive stiffness.

Shear wave (SW) ultrasound elastography, which builds upon traditional elastography, allows quantitative *in vivo* measurement of tissue material properties (Bercoff, 2004). Using the same acoustic radiation forces as B-mode ultrasound, we use the SuperSonic Shear Imagine (Bercoff, 2004), a method that uses multiple ultrasound push beams to induce the SWs and subsequently, to measure the SW speed in muscle. The speed of these SWs is related to material properties, such that SWs travel faster through stiffer tissues. This technique has emerged as a reliable method to estimate material properties in a variety of tissues (Bouillard et al., 2012), including muscle (Bouillard et al., 2012; Eby et al., 2013; Lacourpaille et al., 2012). Several earlier studies have measured SW speed in muscles such as the biceps brachii (Bouillard et al., 2012; Lacourpaille et al., 2012), gastrocnemius (Chernak et al., 2013; Lacourpaille et al., 2012), and vastus lateralis muscles (Lacourpaille et al., 2012) in both healthy individuals and in individuals with neuromuscular dysfunction such as spasticity (Basford et al., 2002; Kwon, 2012; Lee et al., 2015). Using MRI to measure SW speed, Basford et al. observed the shear modulus in resting lateral gastrocnemius muscle of individuals with neuromuscular disease such as childhood poliomyelitis and spastic paraplegia, to be 2.4 times larger than that of non-impaired muscle (Basford et al., 2002). Recently, SW speed in the biceps brachii muscle of the paretic side was found to be on average 69.5% greater than the non-paretic side in stroke survivors (Lee et al., 2015). Greater SW velocities in the gastrocnemius muscles of children with CP were also reported, compared to typically developing children with the ankle at 90° (Kwon, 2012).

Building upon these results, the goal of this study was to evaluate SW speed of the medial gastrocnemius (MG) and tibialis anterior (TA) in children with hemiplegic CP over a range of ankle positions and torques. We hypothesized that SW speed would 1) be greater in the more-affected limb than the less-affected limb of children with hemiplegic CP, 2) increase with muscle stretch as indicated by ankle position and increase with increasing fascicle strain, and 3) increase with decreased ankle range of motion.

2. Methods

2.1 Participants

Eight individuals (five males, three females; mean (SD) age: 9.4 (3.7) yrs; height: 1.31 (0.17) m; body mass: 33.3 (12.8) kg; Gross Motor Function Classification System (GMFCS) Levels: three subjects at I; five subjects at II) participated in the study. Children with CP were recruited from the Rehabilitation Institute of Chicago for participation in this study. Inclusion criteria were a diagnosis of spastic hemiplegic CP by a physician specializing in pediatric rehabilitation medicine, between the ages of 5 and 18 years, able to ambulate with or without walking aids, and no botulinum toxin injections or surgical procedures to MG or TA within the past year. Although the inclusion criteria specified a diagnosis of hemiplegic CP, one subject (S7) had a stroke at five years of age; however, due to similar movement impairments, he was included in the study. The physician also identified which side was the impaired or more-affected side from visual and manual inspection (e.g. muscle weakness,

loss of selective control, increased tone, decreased range of motion, skeletal deformity). The Institutional Review Board of Northwestern University approved all protocols and consent from the subjects was obtained prior to testing.

2.2 Experimental protocol

Ultrasound images were captured over a range of ankle positions. A small rotary actuator, “The IntelliStretch Rehabilitation Robot” (Rehabtek LLC, Glenview, IL) was used to continuously monitor ankle angle and torque throughout the experiment. Each subject was seated in the IntelliStretch with his or her knee in maximum extension and their foot strapped to the device (Fig. 1A). Tracking both knee and ankle positions were important since the MG crosses both joints and knee position will impact the magnitude of MG stretch. Maximum extension was chosen rather than a standardized joint angle to account for different resting muscle lengths. Since resting muscle length is variable among individuals with CP, maximum knee extension would indicate the MG muscle is at its longest length. Thus, this position would be comparable between subjects.

B-mode and SW ultrasound elastography measurements of TA (Fig. 1B) and MG were made with the ankle in five positions (neutral, maximum dorsiflexion, maximum plantarflexion, and two intermediary angles) with the muscles at rest. Intermediary angles were chosen at which torque values were one-third and two-thirds of the torque measured at maximum dorsiflexion and plantarflexion for the initial tested limb. These two torque values were then used for finding the two intermediary angles for the contralateral limb at which the torque values were matched. Three trials in randomized order were performed in each position. Ultrasound images were captured using an Aixplorer Ultrasonography System (SuperSonic Imagine, Aix-en-Provence, France) with a linear transducer array (4-15 MHz, SuperLiner 15-4, Vermon, Tours, France) (Bercoff, 2004). Technical details of this SuperSonic Imagine technology have been described previously (Bercoff, 2004). A customized neoprene sleeve held the transducer in place to minimize translation or tilt of the transducer. The transducer was orientated parallel to the fascicle plane at the mid-belly region of each muscle. The region of interest, from which the SW velocities were measured, was placed over the mid-region of the muscle belly (Fig. 1B). Images were taken separately for the TA and MG of each leg, for a total of 60 trials (2 legs, 2 muscles, 15 trials/muscle). Subjects were instructed to remain relaxed during this study, but to test if muscle activation also increased with ankle position, we monitored electromyography (EMG) signals (Trigno EMG, Delsys, Inc., Boston, MA) from the MG and TA in three subjects. For those three subjects, there was no evidence of increased muscle activity.

2.3 Ultrasound processing

A custom-written software in Matlab (Mathworks, Natick, USA), adapted from the propriety company software, was used in this study. The mean SW speed is calculated from a circular region with varying diameters selected by the experimenter from the 12mm by 12mm region of interest (Fig. 1B). In our software, instead of using the circular region, all the values from the region of interest were used except for areas outside of the muscle belly, which were manually cropped. This way, the maximal area for including SW speed values was achieved. The spatial average of SW speed was then calculated across the cropped

region of interest for each muscle. The company software, Q Box, provides each SW speed with 'quality factor' values that indicates the accuracy of the SW speed measurement. This is related to the cross-correlation algorithm that the company software uses to track the propagation of SWs through the tissue. The mean SW speed is calculated from SW speed values that have a quality factor greater than 0.8. In this study, each image had on average at least 90% of SW speed values that had a quality factor greater than 0.8.

We have previously tested the repeatability and reliability of the SW speed measurements. In these pilot analyses, three unimpaired subjects, were tested twice on separate days. SW speed was reliable and repeatable (ICC=0.932, CV=4.5%). Inter-day reliability of the SuperSonic Imagine technique has also been previously reported (Lacourpaille et al., 2012; Yoshitake et al., 2013).

The B-mode ultrasound images were used to measure muscle thickness and fascicle lengths for the trials at neutral ankle position. Thickness was measured by digitizing the distance between the superficial and deep aponeuroses in the MG and between the superficial and middle aponeuroses in the TA (Lee and Piazza, 2009). An average thickness from five measurements made in the thickest region of the muscle was calculated. Fascicle length was measured by digitizing the fascicle between the superficial and deep aponeuroses. The average fascicle length was calculated from five fascicle length measurements. Fascicle strain was computed by dividing the difference between the fascicle length and the neutral angle fascicle length by the neutral angle fascicle length.

2.4 Statistical analysis

We used an Analysis of Variance to compare the SW speed between the more- and less-affected limbs of the subjects with hemiplegic CP, as diagnosed clinically. SW speed between limbs was compared at neutral ankle angles and for maximum stretch (maximum dorsiflexion for the MG and maximum plantarflexion for the TA). An Analysis of Covariance was conducted to evaluate the influence of ankle torques, angles, and fascicle strain (covariates) on SW speed between the more-affected and less-affected limbs. Regression analyses were conducted to evaluate correlations between SW speed, muscle thickness, fascicle strain, torque, and ankle angle.

3. Results

3.1 Ultrasound measurements

SW speed in the MG and TA of the more-affected limb was higher (MG: S1, S3, S5-S8; TA: S3-S8) than the less-affected limb at neutral angle, 90°, in six of the eight subjects, and was significantly different between limbs: on average 14% and 20% greater in the more-affected than less-affected MG and TA muscles, respectively (MG, more affected: 5.05 (0.55) m/s, less-affected: 4.46 (0.57) m/s, $p=0.024$, Fig. 2; TA, more affected: 3.86 (0.79) m/s, less-affected: 3.22 (0.40) m/s, $p=0.03$) (Fig. 3). At the limits of ankle range of motion, there was no significant difference in SW speed in the MG in maximum dorsiflexion between the two sides (more-affected: 8.55 (2.43) m/s; less-affected: 8.18 (1.94) m/s, $p=0.40$). The SW speed in the TA in maximum plantarflexion was significantly higher in the less-affected limb, by

11% on average (more-affected: 4.56 (0.70) m/s; less-affected: 5.14 (0.89) m/s, $p=0.006$, Fig. 3).

As demonstrated in Figures 4 and 5, SW speed increased in MG and TA with increasing ankle angle, torque, and fascicle strain such that SW speed increased with muscle lengthening and fascicle strain. From the ANCOVA, ankle torque and angle, as well as fascicle strain, had significant effects (all $p<0.001$) on SW velocities for all individuals (Figs. 4 and 5). Figure 4 shows that: 1) MG SW speed increased as ankle torque increased with a linear fit $r^2=0.56$ ($p<0.001$) for the less-affected side and with $r^2=0.45$ ($p<0.001$) for the more affected side, 2) MG SW speed increased as ankle angle increased with a quadratic fit with $r^2=0.82$ ($p<0.001$) and $r^2=0.69$ ($p<0.001$) for the less- and more-affected side, respectively, and 3) MG SW speed increased as fascicle strain increased with a linear fit with $r^2=0.63$ ($p<0.001$) for the less-affected side and $r^2=0.53$ ($p<0.001$) for the more affected side.

The range of SW velocities for the TA was smaller across all subjects and limbs compared to the MG (Figs 3 and 5). Thus, for the TA, the comparison of SW speed versus torque had a linear fit with $r^2=0.06$ ($p=0.001$) and $r^2=0.001$ ($p=0.001$) for the less- and more-affected side, respectively. A comparison between SW speed and angle revealed a quadratic relationship, $r^2=0.35$ ($p<0.001$) and $r^2=0.12$ ($p=0.001$), for the less- and more-affected side, respectively. (Fig.5). SW speed increased as fascicle strain increased for both the less- and more-affected TA with a linear fit $r^2=0.11$ ($p<0.001$) and $r^2=0.07$ ($p=0.001$), respectively.

From the B-mode ultrasound images, muscle thickness and fascicle length, as measured with the ankle at a neutral 90° position, was also significantly reduced on the more-affected limb (Fig. 6). For the MG, muscle thickness of the more-affected limb ($10.2\pm 2.9\text{mm}$) was on average 22% less than the less-affected limb ($13.0\pm 3.1\text{mm}$, $p<0.001$). We observed a greater muscle thickness difference in the TA; the more-affected limb ($5.8\pm 1.3\text{mm}$) was on average 26% less than the less-affected limb ($7.9\pm 1.4\text{mm}$, $p=0.015$). For both muscles and all subjects, there was no significant relationship between SW speed and muscle thickness. Fascicles of the less-affected side were substantially longer on average for both the MG and TA, than the more-affected side with the ankle at neutral angle (Fig. 6). For the MG, the fascicles of the more-affected side ($37.6\pm 8.0\text{mm}$) were 25% shorter than the less-affected side ($50.5 \pm 7.8\text{mm}$, $p = 0.013$). For the TA, the fascicles of the more-affected side ($44.1 \pm 12.1\text{mm}$) were 19% shorter than the less-affected side ($54.3 \pm 12.9\text{mm}$, $p=0.003$).

3.2 Clinical assessments

The more affected side had significantly decreased active range of motion at the ankle (more-affected: $35.9\pm 16.4^\circ$; less-affected: $59.3\pm 12.3^\circ$ $p = 0.039$) compared to the less affected side, but the passive range of motion between the two sides was not significantly different (more-affected: $59.0\pm 9.3^\circ$; less-affected: $64.5\pm 13.7^\circ$ $p = 0.29$). To relate SW speed measurements with clinical assessment, we evaluated the relationship between SW speed and passive and active ankle range of motion. There was no significant correlation between SW speed of the MG or TA and ankle range of motion as indicated by the maximum dorsiflexion angle. There was no significant difference in SW speed between the children with GMFCS Levels I and II.

4. Discussion

Using SW ultrasound elastography, we demonstrated that SWs travel faster in both MG and TA of the more-affected limb of individuals with hemiplegic CP. Moreover, for the MG and TA, SW speed increased as torque, ankle angle, and fascicle strain increased. This work provides further evidence that SW speeds for the MG and TA are dependent upon ankle angle, torque, and fascicle strain. These results suggest that individuals with CP have altered muscle material properties, specifically greater stiffness, which can be quantified with SW elastography.

There are multiple factors that may contribute to increased muscle SW speed in CP. Changes in muscle stiffness are often attributed to altered properties of passive structures within a muscle. In CP spastic muscle, there is evidence of increased extracellular material (Smith et al., 2011), stiffer fibers (Friden and Lieber, 2003; Lieber et al., 2003), and increased collagen content (Smith et al., 2011) in spastic muscle is shown to be correlated with the clinical severity of muscle spasticity (Booth et al., 2001). Titin, a large protein within the sarcomere that is believed to contribute to passive tension (Prado et al., 2005), may also contribute to increased passive stiffness. Recently, fiber and fiber bundle stiffness of the gastrocnemius and soleus muscles of individuals with CP was reported to be stiffer than that of typically developing children (Mathewson et al., 2014).

To provide further insight into changes in muscle composition, future studies should probably also include methods such as calculating the echogenicity from B-mode ultrasound images (Pillen et al., 2009) or using magnetic resonance imaging (Marden et al., 2005; Murphy et al., 1986). Echogenicity is correlated with increased amounts of intramuscular fat or fibrous tissue (Pillen et al., 2009) and is reported to be higher in stroke-impaired muscle (Lee et al., 2015) and in muscle in children with myopathic and neuromuscular disorders (Lamminen et al., 1988; Pillen et al., 2007).

Our finding that SW speed increased with muscle length, as measured by joint angle, and fascicle strain suggests these changes in SW speed were linked to increased passive tension, rather than to active factors, such as muscle activation or reflex hypertonicity. Others have demonstrated that SW speed increases with increasing muscle activation (Bouillard et al., 2012; Chernak et al., 2013; Yoshitake et al., 2013) and recently, shear modulus, as calculated as the SW speed squared, of the gastrocnemius at different lengths during passive conditions was observed to have a similar relationship to that of the normalized force-length relationship (Chernak et al., 2013; Maïsetti et al., 2012). As shown in Figures 4 and 5, SW speed increased as torque, ankle angle, and fascicle strain increased. These relationships are similar to those observed by Chernak et al. (Chernak et al., 2013) and in addition, we present here the first reported relationship between fascicle strain and SW speed as previous reports are of SW speed and joint angle (Chernak et al., 2013; Maïsetti et al., 2012).

Although there was no evidence of increased muscle activity in the three subjects from which we collected EMG data, it is not possible to completely rule out greater baseline EMG due to reflex hypertonicity. Future investigations of SW speed after injection of

botulinum toxin type-A or other paralytic agents may provide insight into the proportion of SW speed due to active factors.

In this evaluation of SW elastography, we focused on a representative population of individuals with CP that visited a clinical center. Future studies examining a larger population and including age and size-matched controls will further inform the clinical use of SW elastography. An investigation with individuals with greater impairment such as significant plantarflexor contracture and a larger range of GMFCS Levels would help determine the relationship between SW speed and functional impairment. In this study, we have used the terms 'less-affected' and 'more-affected' because even in hemiplegic CP, the 'non-affected' limb might be affected, but not at a clinically-detectable or significant level. The SW speeds measured in this study for the less-affected side were comparable to that of typically developing children of similar ages and other studies of healthy MG muscle across different lengths (Chernak et al., 2013; Lacourpaille et al., 2012). Using the same ultrasound system, SW speed of the lateral gastrocnemius muscle in typically developing children was reported to range from 2.77 to 5.52 m/s over the range of 20° plantarflexion to 10° dorsiflexion with an average of 4.20 m/s at 90° ankle angle (Brandenburg et al., 2015). Kwon et al. also reported lower SW speed of the MG in typically developing children (1.3 m/s) compared to children with CP (2.5 m/s) which are comparable to the results reported here (Kwon, 2012).

The muscle thickness and fascicle length results were comparable to many previous studies of the MG and TA of children with CP and typically developing children (Barber et al., 2011; Gao et al., 2011; Legerlotz et al., 2010; Malaiya et al., 2007; Shortland et al., 2002). There has not been a definitive consensus on whether fascicle length is longer or shorter in children with CP compared to typically developing children. The confounding factors include the muscle length at which the fascicles lengths are measured. Fascicle lengths measured at the same joint angle are often compared, including in this study, between groups. However, the muscle length, relative to resting length, is unlikely to be the same between children with CP and typically developing children. Thus, we chose to compare the relationship between SW speed and fascicle strain. In addition, it is important to note that knowing fascicle length is not enough to infer information about muscle mechanics and the force-length property since sarcomeres are the basic units of muscle. A normal length fascicle or fiber can have highly stretched sarcomeres (Foran et al., 2005).

Several important limitations and methodological challenges need to be addressed. In isotropic homogenous materials, SW speed is directly related to Young's Modulus (Royer et al., 2011); however, this is not necessarily true in tissue which is transversely anisotropic (Royer et al., 2011), such as muscle. Previous work has shown SW is related to Young's modulus in muscle (Eby et al., 2013), but that the exact relationship remains unclear, in particular for in vivo passive and active measurements. Thus, we reported SW speed. Moreover, it is currently unclear which specific material properties influence SW propagation. Current and future work of our group and others is focused on determining the relationships between SW velocity and muscle material properties. Additionally, current measurements of SW speed cannot distinguish between the factors that may contribute to increased muscle stiffness such as the extracellular matrix, intracellular proteins, or

reflexively mediated hypertonicity. Coupling these measurements with muscle biopsies and histochemistry will allow evaluation of underlying mechanisms in spastic muscle.

5. Conclusions

Using SW ultrasound elastography, we demonstrated that SWs travel faster in the MG and TA of the more-affected than less affected limb of individuals with unilateral CP. This suggests that the affected muscles have altered material properties, specifically greater stiffness. SW speed was also demonstrated to increase in MG and TA with increasing ankle angle, joint torque, and fascicle strain. By combining traditional B-mode ultrasound with SW elastography, a more thorough evaluation of muscle can be conducted in a muscle-specific, non-invasive, and real-time manner. Characterizing altered muscle properties in individuals with CP is important for understanding the causes of abnormal movement and for guiding treatment planning. These measurements can be beneficial to clinicians as treatment decisions such as surgery or pharmaceutical interventions may differ depending on the underlying muscle impairments.

Acknowledgements

The authors would like to thank Dr. K. Chen for assistance with data collection and use of equipment. This work was funded by NIDDR H133P110013, NIH K12HD073945, and the AACPD Research Grant.

References

- Barber L, Barrett R, Lichtwark G. Passive muscle mechanical properties of the medial gastrocnemius in young adults with spastic cerebral palsy. *Journal of biomechanics*. 2011; 44:2496–2500. [PubMed: 21762920]
- Basford JR, Jenkyn TR, An K-N, Ehman RL, Heers G, Kaufman KR. Evaluation of healthy and diseased muscle with magnetic resonance elastography. *Archives of Physical Medicine and Rehabilitation*. 2002; 83:1530–1536. [PubMed: 12422320]
- Bercoff JT, Mickael, Fink Mathias. Supersonic shear imaging - a new technique for soft tissue elasticity mapping. *IEEE transactions on ultrasonics, ferroelectrics, and frequency control*. 2004; 51:396–409.
- Booth CM, Cortina-Borja MJ, Theologis TN. Collagen accumulation in muscles of children with cerebral palsy and correlation with severity of spasticity. *Developmental medicine and child neurology*. 2001; 43:314–320. [PubMed: 11368484]
- Bouillard K, Nordez A, Hodges PW, Cornu C, Hug F. Evidence of changes in load sharing during isometric elbow flexion with ramped torque. *Journal of biomechanics*. 2012; 45:1424–1429. [PubMed: 22406469]
- Brandenburg JE, Eby SF, Song P, Zhao H, Landry BW, Kingsley-Berg S, Bamlet WR, Chen S, Sieck GC, An K-N. Feasibility and Reliability of Quantifying Passive Muscle Stiffness in Young Children by Using Shear Wave Ultrasound Elastography. *Journal of Ultrasound in Medicine*. 2015; 34:663–670. [PubMed: 25792582]
- Chardon, MK.; Suresh, NL.; Rymer, WZ. An evaluation of passive properties of spastic muscles in hemiparetic stroke survivors, *Engineering in Medicine and Biology Society (EMBC). 2010 Annual International Conference of the IEEE; IEEE; 2010. p. 2993-2996.*
- Chernak LA, DeWall RJ, Lee KS, Thelen DG. Length and activation dependent variations in muscle shear wave speed. *Physiological measurement*. 2013; 34:713–721. [PubMed: 23719230]
- Eby SF, Song P, Chen S, Chen Q, Greenleaf JF, An KN. Validation of shear wave elastography in skeletal muscle. *Journal of biomechanics*. 2013; 46:2381–2387. [PubMed: 23953670]

- Foran JR, Steinman S, Barash I, Chambers HG, Lieber RL. Structural and mechanical alterations in spastic skeletal muscle. *Developmental Medicine & Child Neurology*. 2005; 47:713–717. [PubMed: 16174321]
- Friden J, Lieber RL. Spastic muscle cells are shorter and stiffer than normal cells. *Muscle & nerve*. 2003; 27:157–164. [PubMed: 12548522]
- Gage, JR. The identification and treatment of gait problems in cerebral palsy. 2nd ed.. Mac Keith Press; London: 2009.
- Gao F, Zhao H, Gaebler-Spira D, Zhang L-Q. In vivo evaluations of morphologic changes of gastrocnemius muscle fascicles and achilles tendon in children with cerebral palsy. *American Journal of Physical Medicine & Rehabilitation*. 2011; 90:364–371. [PubMed: 21765255]
- Ito J, Araki A, Tanaka H, Tasaki T, Cho K, Yamazaki R. Muscle histopathology in spastic cerebral palsy. *Brain & development*. 1996; 18:299–303. [PubMed: 8879649]
- Kwon DP, Young Gi, Lee Sung Uk, Chung Inbum. Spastic cerebral palsy in children : dynamic sonoelastographic findings of medial gastrocnemius. *Radiology*. 2012; 263:794–801. [PubMed: 22495685]
- Lacourpaille L, Hug F, Bouillard K, Hogrel JY, Nordez A. Supersonic shear imaging provides a reliable measurement of resting muscle shear elastic modulus. *Physiological measurement*. 2012; 33:N19–28. [PubMed: 22370174]
- Lamminen A, Jääskeläinen J, Rapola J, Suramo I. High-frequency ultrasonography of skeletal muscle in children with neuromuscular disease. *Journal of Ultrasound in Medicine*. 1988; 7:505–509. [PubMed: 3054144]
- Lee SS, Piazza SJ. Built for speed: musculoskeletal structure and sprinting ability. *The Journal of experimental biology*. 2009; 212:3700–3707. [PubMed: 19880732]
- Lee SS, Spear S, Rymer WZ. Quantifying changes in material properties of stroke-impaired muscle. *Clinical Biomechanics*. 2015; 30:269–275. [PubMed: 25638688]
- Legerlotz K, Smith HK, Hing WA. Variation and reliability of ultrasonographic quantification of the architecture of the medial gastrocnemius muscle in young children. *Clinical physiology and functional imaging*. 2010; 30:198–205. [PubMed: 20184623]
- Lieber RL, Runesson E, Einarsson F, Fridén J. Inferior mechanical properties of spastic muscle bundles due to hypertrophic but compromised extracellular matrix material. *Muscle & nerve*. 2003; 28:464–471. [PubMed: 14506719]
- Magid A, Law DJ. Myofibrils bear most of the resting tension in frog skeletal muscle. *Science*. 1985; 230:1280–1282. [PubMed: 4071053]
- Maïsetti O, Hug F, Bouillard K, Nordez A. Characterization of passive elastic properties of the human medial gastrocnemius muscle belly using supersonic shear imaging. *Journal of biomechanics*. 2012; 45:978–984. [PubMed: 22326058]
- Malaiya R, McNee AE, Fry NR, Eve LC, Gough M, Shortland AP. The morphology of the medial gastrocnemius in typically developing children and children with spastic hemiplegic cerebral palsy. *Journal of electromyography and Kinesiology*. 2007; 17:657–663. [PubMed: 17459729]
- Marden FA, Connolly AM, Siegel MJ, Rubin DA. Compositional analysis of muscle in boys with Duchenne muscular dystrophy using MR imaging. *Skeletal radiology*. 2005; 34:140–148. [PubMed: 15538561]
- Mathewson MA, Chambers HG, Girard PJ, Tenenhaus M, Schwartz AK, Lieber RL. Stiff muscle fibers in calf muscles of patients with cerebral palsy lead to high passive muscle stiffness. *Journal of Orthopaedic Research*. 2014; 32:1667–1674. [PubMed: 25138654]
- Murphy WA, Totty W, Carroll J. MRI of normal and pathologic skeletal muscle. *American journal of roentgenology*. 1986; 146:565–574. [PubMed: 3484872]
- Park G-Y, Kwon DR. Sonoelastographic evaluation of medial gastrocnemius muscles intrinsic stiffness after rehabilitation therapy with botulinum toxin a injection in spastic cerebral palsy. *Archives of physical medicine and rehabilitation*. 2012; 93:2085–2089. [PubMed: 22776155]
- Pillen S, van Dijk JP, Weijers G, Raijmann W, de Korte CL, Zwarts MJ. Quantitative gray-scale analysis in skeletal muscle ultrasound: a comparison study of two ultrasound devices. *Muscle & nerve*. 2009; 39:781–786. [PubMed: 19301363]

- Pillen S, Verrips A, Van Alfen N, Arts I, Sie L, Zwarts M. Quantitative skeletal muscle ultrasound: diagnostic value in childhood neuromuscular disease. *Neuromuscular Disorders*. 2007; 17:509–516. [PubMed: 17537635]
- Ponten EM, Stal PS. Decreased capillarization and a shift to fast myosin heavy chain IIX in the biceps brachii muscle from young adults with spastic paresis. *Journal of the neurological sciences*. 2007; 253:25–33. [PubMed: 17196619]
- Prado LG, Makarenko I, Andresen C, Krüger M, Opitz CA, Linke WA. Isoform diversity of giant proteins in relation to passive and active contractile properties of rabbit skeletal muscles. *The Journal of general physiology*. 2005; 126:461–480. [PubMed: 16230467]
- Royer D, Gennisson JL, Deffieux T, Tanter M. On the elasticity of transverse isotropic soft tissues (L). *J Acoust Soc Am*. 2011; 129:2757–2760. [PubMed: 21568379]
- Shortland AP, Harris CA, Gough M, Robinson RO. Architecture of the medial gastrocnemius in children with spastic diplegia. *Developmental medicine and child neurology*. 2002; 44:158–163. [PubMed: 12005316]
- Sinkjær T, Magnussen I. Passive, intrinsic and reflex-mediated stiffness in the ankle extensors of hemiparetic patients. *Brain*. 1994; 117:355–363. [PubMed: 8186961]
- Sinkjær T, Toft E, Andreassen S, Hornemann BC. Muscle stiffness in human ankle dorsiflexors: intrinsic and reflex components. *Journal of neurophysiology*. 1988; 60:1110–1121. [PubMed: 3171659]
- Sinkjær T, Toft E, Larsen K, Andreassen S, Hansen HJ. Non-reflex and reflex mediated ankle joint stiffness in multiple sclerosis patients with spasticity. *Muscle & nerve*. 1993; 16:69–76. [PubMed: 8423835]
- Smith LR, Lee KS, Ward SR, Chambers HG, Lieber RL. Hamstring contractures in children with spastic cerebral palsy result from a stiffer extracellular matrix and increased in vivo sarcomere length. *The Journal of physiology*. 2011; 589:2625–2639. [PubMed: 21486759]
- Yeargin-Allsopp M, Van Naarden Braun K, Doernberg NS, Benedict RE, Kirby RS, Durkin MS. Prevalence of cerebral palsy in 8-year-old children in three areas of the United States in 2002: a multisite collaboration. *Pediatrics*. 2008; 121:547–554. [PubMed: 18310204]
- Yoshitake Y, Takai Y, Kanehisa H, Shinohara M. Muscle shear modulus measured with ultrasound shear-wave elastography across a wide range of contraction intensity. *Muscle & nerve*. 2013

Highlights

- Shear waves travel faster in gastrocnemius of more-affected limb in hemiplegic cerebral palsy
- Shear wave velocity increases as torque, angle, and strain increase
- Muscle material properties may be altered in cerebral palsy muscle

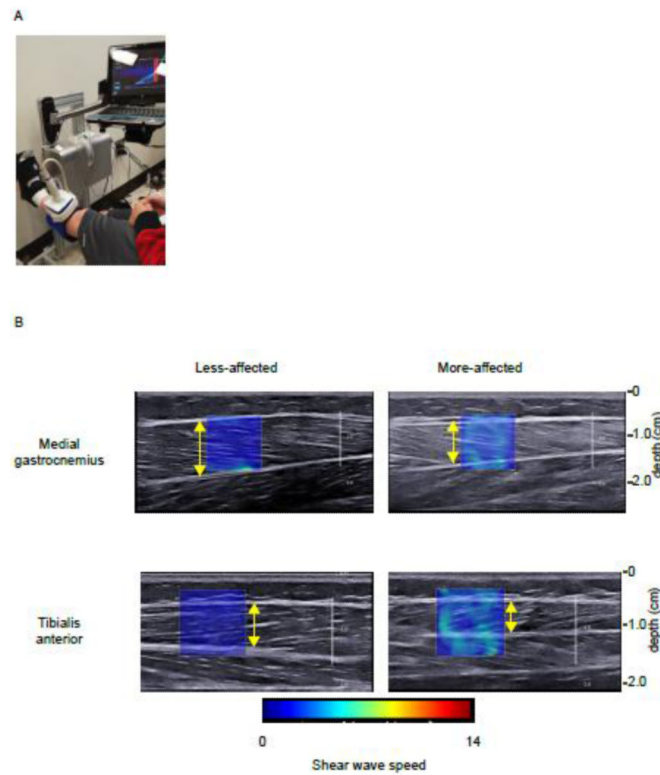


Figure 1.

A) Experimental set-up: the subject is seated with their knee in full extension and foot strapped to the IntelliStretch, a device which moves the ankle and records ankle angle and torque. The ultrasound transducer is fixed to the subject's limb (in this picture, the TA is being imaged) by a custom-holder. **B)** Representative ultrasound images (SW speed map superimposed on the B-mode image) of the less-affected and more-affected MG and TA at neutral ankle angle. The shear wave speed is greater in the more-affected limb. Yellow arrows indicate measurement of muscle thickness.

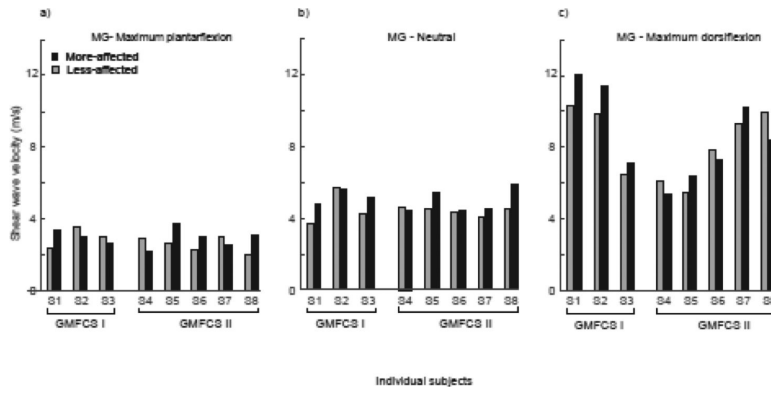


Figure 2. Mean SW speed of the less-affected (grey bars) and more-affected (black bars) MG at a) maximum plantarflexion, b) 90° neutral ankle angle, and c) maximum dorsiflexion for the individual subjects, grouped by GMFCS Levels I and II.

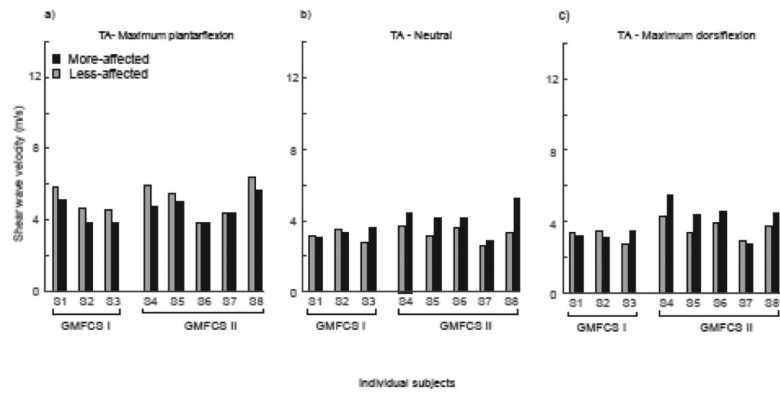


Figure 3. Mean SW speed of the less-affected (grey bars) and more-affected (black bars) TA at a) maximum plantarflexion, b) 90° neutral ankle angle, and c) maximum dorsiflexion for the individual subjects, grouped by GMFCS Levels I and II.

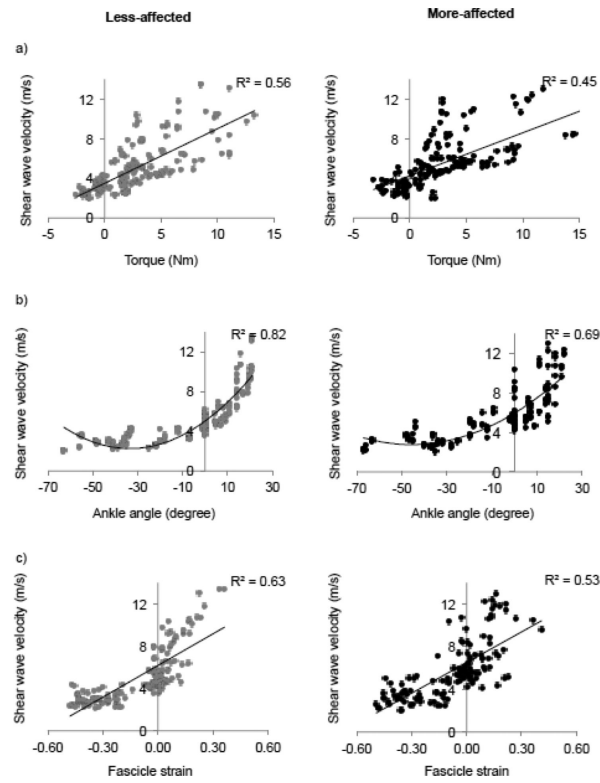


Figure 4.

SW speed of the MG plotted against a) torque, b) angle, and c) fascicle strain for all trials of the less-affected side (grey) and more affected side (black). Linear fits are shown for SW speed versus torque and fascicle strain. A quadratic fit is shown for SW speed versus ankle angle.

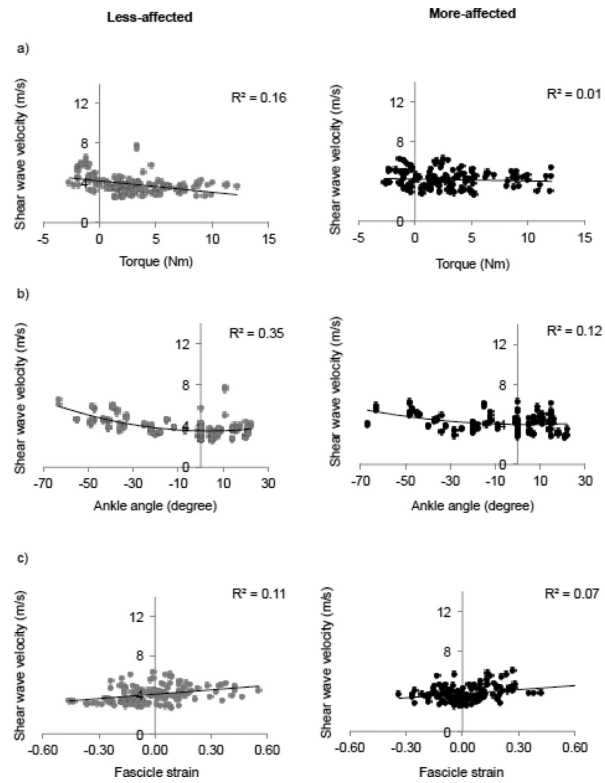


Figure 5. SW speed of the tibialis anterior plotted against a) ankle torque, b) ankle angle, and c) fascicle strain for all trials of the less-affected side (grey) and more affected side (black). Linear fits are shown for SW speed versus torque and fascicle strain. A quadratic fit is shown for SW speed versus ankle angle.

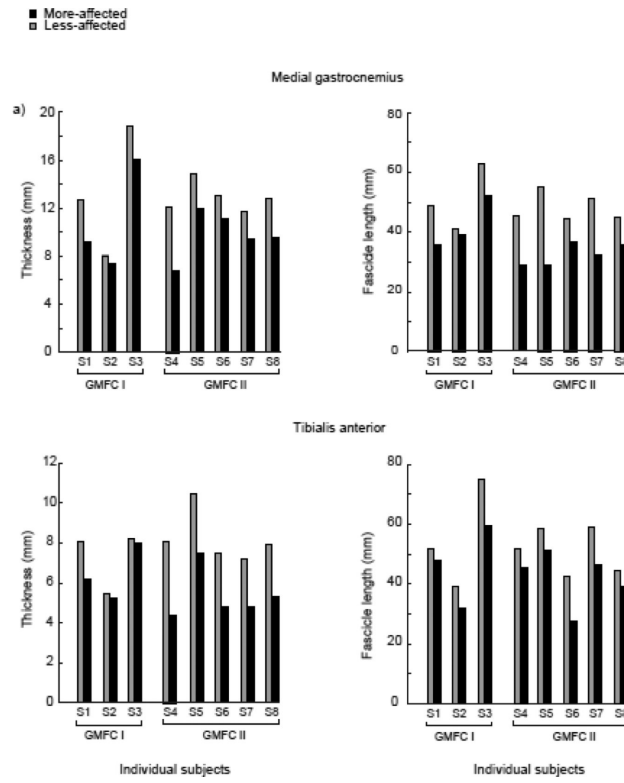


Figure 6. Mean muscle thickness and fascicle length of the less-affected (grey bars) and more-affected (black bars) MG (top) and TA (bottom) for individual subjects at neutral ankle angle. Subjects are grouped by GMFCS Levels I and II.